Polarization-based Decorrelation of Transparent Layers: The Inclination Angle of an Invisible Surface

Yoav Y. Schechner Joseph Shamir Nahum Kiryati[†]

Department of Electrical Engineering,
Technion - Israel Institute of Technology,
Haifa, Israel 32000
yoavs@tx.technion.ac.il
jsh@ee.technion.ac.il

[†]Dep. of Electrical Engineering - Systems,
Faculty of Engineering, Tel-Aviv University,
Ramat Aviv, Israel 69978
nk@eng.tau.ac.il

Abstract

When a transparent surface is present between an observer and an object, an image reflected by the surface may be superimposed on the image of the observed object. We present a new approach to recover the scenes (layers) and to classify which is the reflected/transmitted one, based on imaging through a polarizing filter at two orientations. Estimates of the separate layers are obtained by weighted pixel-wise differences of these images, inverting the image formation process. However, the weights depend on the angle of incidence, hence on the inclination of the transparent (invisible) surface. This angle is estimated by seeking the angle-value which (through the weights) leads to decorrelation of the estimated layers. Experimental results, obtained using real photos of actual objects, demonstrate the success of angle estimation and consequent layer separation and labeling. The method is shown to be superior to earlier methods where only raw optical data was used.

1. Introduction

In the computer vision and image processing fields, it has usually been assumed that at each point of the image the intensity is single valued. However, the situation in which several (typically two) linearly superimposed contributions exist is often encountered in real-world scenes. For example [4, 8, 10], looking out of a car (or room) window, we see both the outside world (termed *real object* [6, 7, 8]), and a semi-reflection of the objects inside, termed *virtual objects* (Fig. 1). The term *transparent layers* has been used to describe such situations [2]. The combination of several unrelated layers is likely to degrade the ability to analyze and understand them (for example, it can certainly confuse autofocusing devices [8]). The detection of the phenomenon is of importance itself, since it indicates the presence of a clear (invisible), transparent surface in front of the camera, at a distance closer than the actual imaged objects [6, 8].

Earlier approaches to reconstruct each of the layers relied mainly on motion [2], stereo [9], and focus [8]. These methods essentially assume that the superimposed layers lie at significantly different optical distances from the camera [8], and the reconstruction of the low spatial frequency components was ill conditioned [8] (while the DC component was ill posed). Other fundamental ambiguities in the solutions obtained by motion and stereo were discussed in [9, 12].

An approach based on polarization can avoid these problems. Polarimetric imaging has recently drawn interest [5, 11, 14], particularly for removal of specular reflections superimposed on diffuse scattering from opaque surfaces [5, 13]. Suppressing the virtual layer by incorporating a polarizer into the imaging system is a common photographic technique [10]. Some previous works attempted to remove the virtual layer by using just the raw output of a polarization analyzer (Fig. 1) in front of the camera [4, 6]. These methods suggested taking several images of the scene at different states of the polarizer, and picking one of them as the reconstruction of the real layer. However, optical filtering eliminates the reflected (virtual) layer only at a specific incidence angle, called the *Brewster angle* [1, 10], which is $\approx 56^{o}$ for glass (and at which good filtering was demonstrated in [6]). Away from this angle, polarization filtering may improve the visibility of the real object, but cannot eliminate the crosstalk with the virtual layer. Independent components analysis of polarization filtered images was used for this purpose, and demonstrated the potential of polarization as an initial step for separation achieved by signal post processing [3], but the intensities are evaluated up to an unknown factor.

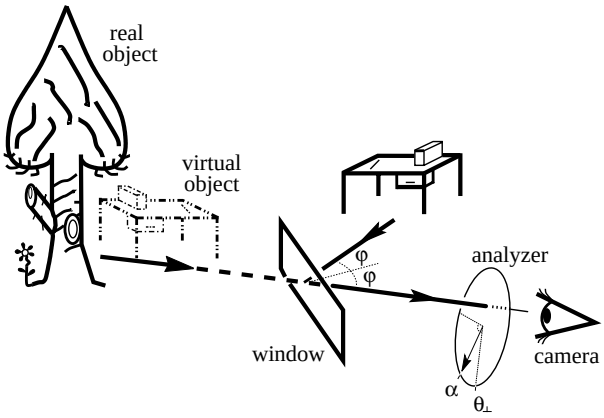

Figure 1. The image of a real object is partly transmitted through a transparent window inclined at an angle φ. The window also creates a virtual image by partly reflecting the image of another object. The combined scene is viewed through a polarization analyzer (filter) at angle α. The plane of incidence includes the incident ray and the normal to the window. The best transmission of the polarization component perpendicular to this plane is when the analyzer is oriented at some value of α denoted $\theta_\perp$.

The most significant disadvantage of the previous works is that they could not determine which of the reconstructed images is of the real object and which is of the virtual one (beside Ref. [6] which attempted the use of the raw images to determine the real layer, and Ref. [7] where the surface had to be curved). Moreover, they did not extract information about the invisible semi-reflecting surface itself, in particular, the angle of incidence (AOI) remained unknown.

In this work we suggest and demonstrate a novel method for separation of the transparent layers and their automatic labeling as virtual or real, together with determination of the angle of incidence (the inclination angle of the invisible semi-reflecting surface). It is based on the physical image formation process, i.e., the combination of two image sources, when viewed through a polarization analyzer. Internal (secondary) reflections within two-surfaced reflecting media (e.g., glass windows) are taken into account.

Initial separation is obtained using the raw output of a polarization analyzer (filter) in front of the camera. Weighted differences between the acquired images yield estimates of the images of the real and the virtual objects. The weights are derived from the reflection and transmission processes determined by the optical properties of the transparent interface. These properties depend on the geometry of the setup, in particular, the angle of incidence (inclination). To estimate it, we seek the weights that lead to *decorrelation* of the estimated layers, based on the assumption that the real object is unrelated to the virtual one.

In contrast to simplistic use of a polarizer, the presented approach allows operation away from Brewster's angle and gives far better results than those achievable by using only raw optical data. Unlike methods that rely on stereo, motion or defocus, it is not ill-conditioned at the low frequencies, it resolves the DC component, and labels the layers as virtual/real. It does not require the layers to have different depths or motion fields.

2. Image formation

The ray incident on a surface (e.g., a face of a window) is partly reflected from the surface, and partly transmitted through it (Fig. 2). All rays lie in the *plane of incidence* (POI). We divide the intensity to two components: $I_{||}$, for which the polarization is *parallel* to the POI, and $I_\perp$, for which the polarization is *perpendicular* to it. Each component has, respectively, reflectivities $R_{||}, R_\perp$ and transmissivities $T_{||}, T_\perp$.

For a single-surface medium (e.g., water in a lake), the reflectivities are [1]

$$R_{||} = \frac{\tan^2(\varphi - \varphi')}{\tan^2(\varphi + \varphi')} \quad , \quad R_\perp = \frac{\sin^2(\varphi - \varphi')}{\sin^2(\varphi + \varphi')} \quad , \qquad (1)$$

where φ is the AOI. φ' is the angle of the ray refracted within the medium (Fig. 2), which is related to φ by Snell's law [1]. Cases of reflection from double-surfaced media are, however, by far more common. Typical examples are glass or polycarbonate windows and covers of pictures. Eqs. (1) also apply to a ray passing from the dense medium (e.g. glass) to the air. As the light ray within the window is refracted to the air at the back surface (Fig. 2), part of it is reflected back to the front surface, from which refraction occurs again, and so on. For each polarization component the total reflectivity is

$$\tilde{R} = R + T^2 R \sum_{l=0}^{\infty} (R^2)^l \quad . \qquad (2)$$

We neglected the absorption within the medium, and assumed that the spatial shift between the significant reflection orders is small relative to the variations in the image. The latter assumption usually holds since, due to the typically small value of R, only the first two orders are significant and since most parts of a typical image are smooth. Thus, the total reflectivities are

$$\tilde{R}_{||} = \frac{2}{1 + R_{||}} R_{||} \quad , \quad \tilde{R}_\perp = \frac{2}{1 + R_\perp} R_\perp \quad , \qquad (3)$$

and the transmissivities are

$$\tilde{T}_{||} = \frac{1 - R_{||}}{1 + R_{||}} = 1 - \tilde{R}_{||} \quad , \quad \tilde{T}_\perp = \frac{1 - R_\perp}{1 + R_\perp} = 1 - \tilde{R}_\perp \quad . \qquad (4)$$

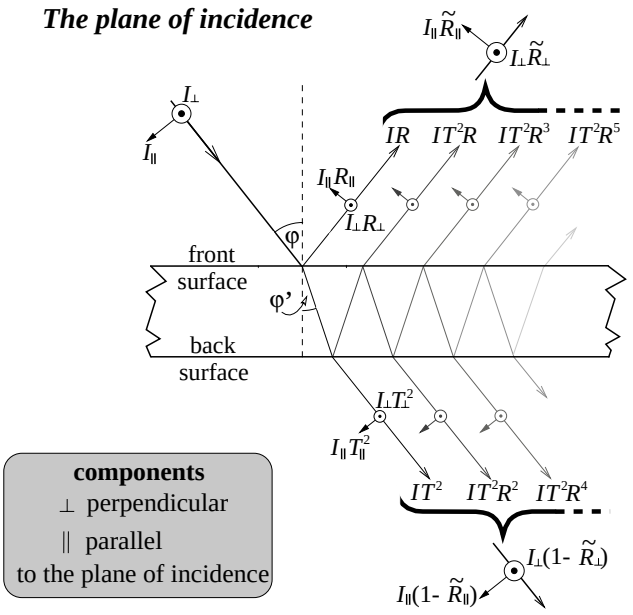

Figure 2. Each component of a light ray incident on any of the window surfaces undergoes reflection and refraction (transmission) with coefficients R and T, respectively. Internal reflections within the window give rise to orders of reflected/transmitted rays with decreasing intensities.

We define the *polarizing effect* (PE) of reflection by the degree of polarization it induces on unpolarized light. For a window it is $\mathrm{PE}_R \equiv |\tilde{R}_{\perp} - \tilde{R}_{||}|/|\tilde{R}_{\perp} + \tilde{R}_{||}|$. As in a single-surface medium, it is full ($\mathrm{PE}_R = 1$) at the Brewster angle, in which the parallel component vanishes [1]. It is zero for 0^o and 90^o. For transmission $\mathrm{PE}_T \equiv |\tilde{T}_{\perp} - \tilde{T}_{||}|/|\tilde{T}_{\perp} + \tilde{T}_{||}|$. It is easy to show that

$$\frac{\mathrm{PE}_T}{\mathrm{PE}_R} = \frac{\tilde{R}_{\mathrm{av}}}{\tilde{T}_{\mathrm{av}}} \quad , \tag{5}$$

where $\tilde{R}_{\mathrm{av}} = (\tilde{R}_{\perp} + \tilde{R}_{||})/2$ and $\tilde{T}_{\mathrm{av}} = (\tilde{T}_{\perp} + \tilde{T}_{||})/2$ are the reflectivity and transmissivity of unpolarized light, respectively. Therefore, *neglecting the degree of polarization induced on the transmitted light (*PE_T*) is equivalent to neglecting the reflection phenomenon (which is invalid in the cases discussed in this work).*

Let I_T be the intensity (at a certain pixel) of the image of the real object without the window. Let I_R be the intensity (at the same pixel) of the image of the virtual object, had there been a perfect mirror instead of the window. For an arbitrary cylindrical coordinate system, whose axis is parallel to the optical axis of the camera, let $\theta_{\perp}$ be the orientation of the polarization analyzer for best transmission of the component perpendicular to the POI. Generally, the orientation of the analyzer is some angle, α. Assuming initially unpolarized natural light, the contribution of the reflected scene is

$$f_R(\alpha) = \frac{I_R}{2}[\tilde{R}_{\perp}\cos^2(\alpha - \theta_{\perp}) + \tilde{R}_{||}\sin^2(\alpha - \theta_{\perp})] \tag{6}$$

and the contribution of the transmitted scene is

$$f_T(\alpha) = \frac{I_T}{2}[\tilde{T}_{\perp}\cos^2(\alpha - \theta_{\perp}) + \tilde{T}_{||}\sin^2(\alpha - \theta_{\perp})] \ . \tag{7}$$

The total intensity is the sum of these contributions,

$$f(\alpha) = \left(\frac{f_{\perp} + f_{||}}{2}\right) + \left(\frac{f_{\perp} - f_{||}}{2}\right)\cos[2(\alpha - \theta_{\perp})] \ , \tag{8}$$

where

$$f_{\perp} = f(\theta_{\perp}) = (I_R\tilde{R}_{\perp}/2 + I_T\tilde{T}_{\perp}/2) \tag{9}$$

$$f_{||} = f(\theta_{\perp} + 90^o) = (I_R\tilde{R}_{||}/2 + I_T\tilde{T}_{||}/2) \ . \tag{10}$$

Note that $f_{\perp} - f_{||} = 0.5(\tilde{R}_{\perp} - \tilde{R}_{||})\,(I_R - I_T)$. Thus, if $I_T = I_R$, the light leaving the reflecting medium (Eq. (8)) is unpolarized. Since $R_{\perp} \geq R_{||}$ [1], it can be shown that $\tilde{R}_{\perp} \geq \tilde{R}_{||}$. Thus, if the real object is brighter than the virtual one ($I_T > I_R$, e.g., when looking out of the room window during daylight), the intensity $f(\alpha)$ would be *minimal* at $\alpha = \theta_{\perp}$. Thus the polarization of the transmitted light, rather than the reflected one, may be dominant in the determination of the overall polarization. Hence, generally one cannot associate $\theta_{\perp}$ with the highest output of the polarization analyzer when imaging transparent scenes.

3. Reconstruction

3.1. For a given angle of incidence

Suppose now that the geometry of the setup, that is, the POI (hence $\theta_{\perp}$) and the AOI φ, is known or estimated. Note that $f_{\perp}$ and $f_{||}$ are not sensitive to small errors in the estimation of $\theta_{\perp}$, since

$$\left.\frac{\partial f}{\partial \theta_{\perp}}\right|_{\alpha=\theta_{\perp},\theta_{\perp}+90^o} = 0 \ . \tag{11}$$

In this case $\tilde{R}_{\perp}(\varphi)$ and $\tilde{R}_{||}(\varphi)$ are known. Thus Eqs. (9,10) together with (4) yield

$$\hat{I}_T(\varphi) = \left[\frac{2\tilde{R}_{\perp}(\varphi)}{\tilde{R}_{\perp}(\varphi) - \tilde{R}_{||}(\varphi)}\right] f_{||} - \left[\frac{2\tilde{R}_{||}(\varphi)}{\tilde{R}_{\perp}(\varphi) - \tilde{R}_{||}(\varphi)}\right] f_{\perp} \tag{12}$$

and

$$\hat{I}_R(\varphi) = \left[\frac{2 - 2\tilde{R}_{||}(\varphi)}{\tilde{R}_{\perp}(\varphi) - \tilde{R}_{||}(\varphi)}\right] f_{\perp} - \left[\frac{2 - 2\tilde{R}_{\perp}(\varphi)}{\tilde{R}_{\perp}(\varphi) - \tilde{R}_{||}(\varphi)}\right] f_{||} \tag{13}$$

Hence if the AOI is the Brewster angle [1] (for which $\tilde{R}_{||} = 0$), $\hat{I}_T$ can be directly associated with $f_{||}$, as demonstrated in [6]. However, even at that angle, $\hat{I}_R$ is not proportional to $f_\perp - f_{||}$, in contrast to [6]. In any case, operation at Brewster's angle is a rare situation, and one should generally use Eqs. (12,13). The reconstructions become unstable as $(\tilde{R}_\perp - \tilde{R}_{||}) \to 0$, that is, at very low or high AOI.

Mechanical rotation of the analyzer causes small image distortions, leading to false polarization readings at image edges [5, 14]. Here, this results in false edges in the reconstructed layer in locations where true edges exist in the other layer. To mitigate that, we align the raw images such that, locally, the gradients in the resulting reconstructed (difference) images are minimized. No blurring operator is used. It turns out that small local translations lead to better results than a global translation. Note that the presence of genuine edges is typically preserved by this alignment process.

3.2. Estimating the angle of incidence

Changing the analyzer's angle α modulates sinusoidally the intensity at each point (8). This modulation is determined by the point intensities I_R and I_T, and by the reflection coefficients - which in turn depend on the AOI, φ. Since I_R and I_T are unknown, pointwise data analysis provides little information (if at all) on the AOI.

To estimate the AOI, an assumption related to multiple points is needed. *We assume that the real and virtual layers are uncorrelated.* This is reasonable since they usually originate from unrelated scenes.

Inserting Eqs. (9,10), that are based on the true AOI $\varphi_{\rm true}$, into Eqs. (12,13), which assume φ, we obtain that

$$\begin{aligned} \hat{I}_T(\varphi) &= (1-\rho)I_T + \rho I_R \\ \hat{I}_R(\varphi) &= (1-\tau)I_R + \tau I_T \ , \end{aligned} \tag{14}$$

where

$$\rho(\varphi_{\rm true}, \varphi) = \frac{\tilde{R}_\perp(\varphi)\tilde{R}_{||}(\varphi_{\rm true}) - \tilde{R}_\perp(\varphi_{\rm true})\tilde{R}_{||}(\varphi)}{\tilde{R}_\perp(\varphi) - \tilde{R}_{||}(\varphi)} \tag{15}$$

$$\tau(\varphi_{\rm true}, \varphi) = \frac{\tilde{T}_\perp(\varphi)\tilde{T}_{||}(\varphi_{\rm true}) - \tilde{T}_\perp(\varphi_{\rm true})\tilde{T}_{||}(\varphi)}{\tilde{T}_\perp(\varphi) - \tilde{T}_{||}(\varphi)} \ . \tag{16}$$

Loosely speaking, for a range of values of φ traces of the virtual layer will remain in $\hat{I}_T$, resulting in positive correlation between the estimated layers. For other values of φ negative traces of the virtual layer will be left in $\hat{I}_T$, leading to a negative correlation between the estimated layers. By using the correct AOI in Eqs. (12,13) zero correlation between the estimated images is obtained.

Our approach is thus to search for the zero crossing of the correlation between the estimated images

$$\hat{\varphi} = \{\varphi \ : \ Corr[\hat{I}_T(\varphi), \hat{I}_R(\varphi)] = 0\} \ . \tag{17}$$

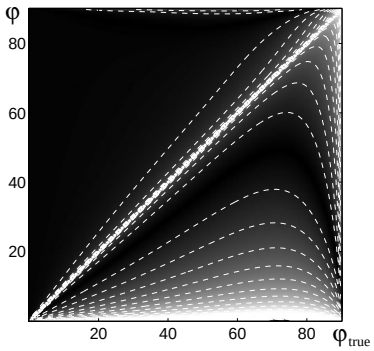

Figure 3. The brightness depicts $|\log|\tau(1-\rho)||$. Zeros of $\tau(1-\rho)$ appear only for $\varphi_{\rm true} = \varphi$.

For any images p and q the cross-correlation is

$$Corr(p,q) = Cov(p,q)/\sqrt{Var(p)\cdot Var(q)} \tag{18}$$

where Var denotes the (spatial) variance. The covariance is estimated in the N-pixels images by

$$Cov(p,q) \simeq \langle p - \mu_p \ , \ q - \mu_q \rangle / N \ , \tag{19}$$

where μ_p is the mean of p. Of course, the zero crossing of the correlation occurs at the zero crossing of the cross-covariance (19), which can also be used to estimate φ. However, note that assuming a constant 'image' as a solution for any layer will satisfy the zero covariance criterion. To reject such possibilities the zero correlation criterion is used. Assuming no correlation between I_R and I_T,

$$Cov(\hat{I}_T, \hat{I}_R) = \tau(1-\rho)Var(I_T) + \rho(1-\tau)Var(I_R) \ . \tag{20}$$

If $\varphi = \varphi_{\rm true}$, then $\rho, \tau = 0$, nulling Eq. (20). Other than in this case, $[\tau(1-\rho)]$ has no zero (Fig. 3), so we can write Eq. (20) as

$$Cov(\hat{I}_T, \hat{I}_R) = \tau(1-\rho)Var(I_R)\left[\frac{Var(I_T)}{Var(I_R)} - \eta\right] \ , \tag{21}$$

where

$$\eta(\varphi_{\rm true}, \varphi) = -\frac{\rho(1-\tau)}{\tau(1-\rho)} \ . \tag{22}$$

Thus, beside the wanted zero-crossing, a zero value of the cross-covariance at a wrongly assumed AOI is possible if and only if $\eta > 0$. We note that if φ is allowed to take values arbitrarily close to 90^o, η can take any positive value. Thus if φ is not bounded by some practical limit, the ambiguity is inevitable for any combination of I_R and I_T. The white domains in Fig. 4 mark the range of AOI on glass for which the possibility of error exists. Note that if it is *a priori* known that the AOI $\varphi_{\rm true}$ is smaller than the Brewster angle, the ambiguity is removed since in these cases

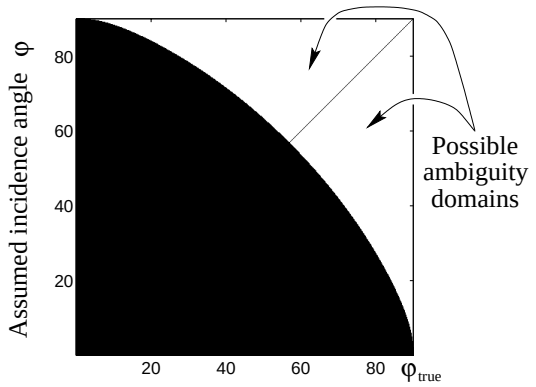

Figure 4. For each $\varphi_{\rm true}$ there are domains (white) where a zero of the correlation exists at a wrong angle (beside the correct one).

Fig. 4 indicates that the wrong angle of decorrelation will always be at $\varphi > \varphi_{\rm true}$. Generally, possible ways to bypass this problem may be based on comparison of the results obtained for different image parts having different variances, or for different color bands, or for shifts between the images prior to the correlation estimation.

An alternative method for estimating the AOI, can be based on the assumption that the statistical dependence of the real and virtual layers is small. Thus, if the layers are correctly separated, each of the estimates contains a minimum of information about the other. The use of mutual information as a criterion for separation is now being studied.

4. Reconstruction experiment

We imaged several objects through an upright glass window. The window semi-reflected another scene. The combined scene is shown (contrast-stretched for clarity, as are all the images here) in Fig. 5(a). The optical distance between the camera and both scenes was $\approx 3.5m$. A linear polarizer was rotated in front of the camera between consecutive image acquisitions. For good demonstration quality, 5 frames were averaged at each analyzer state.

The POI was horizontal, thus it was easy to obtain $\theta_\perp$ and take images of $f_\perp$ and $f_{||}$[1], shown in Fig. 5. The reflected layer is attenuated by the polarizer in $f_{||}$. Still, a significant disturbance due to this scene remains since $\varphi_{\rm true} = 27.5^o \pm 3^0$ was far from the Brewster angle. Thus optics alone does not solve the problem.

The AOI φ to be estimated, was assumed to be between 5^o and 85^o (to avoid instabilities at the singular angles 0^o and 90^o). For each assumed angle, the cross-correlation between the images was estimated. At $\varphi = 27^o$ the estimated layers are decorrelated (Fig. 6). This is in excellent agreement with the angle used in the physical experimental setup. A second zero-crossing of the correlation coefficient exists at 84^o. This result is also in agreement with the theory, since for this φ_{true}, the threshold for the appearance of this crossing (Fig. 4) is 80^o.

[1]More details, and the raw images database can be linked through $http://www.ee.technion.ac.il/\sim yoavs/PUBLICATIONS$.

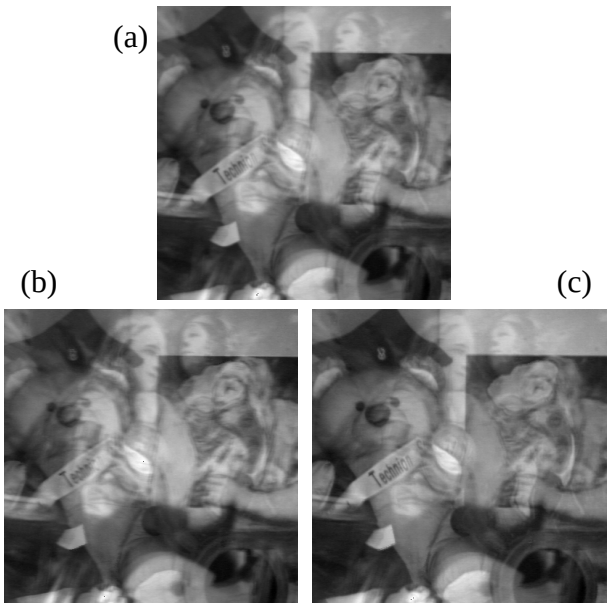

Figure 5. (a): The combined scene. (b): $f_\perp$. (c): $f_{||}$. Although the reflected component is weaker in $f_{||}$, the image is still unclear.

We operated Eqs. (12,13) on each point in the images shown in Figs. 5(b,c) using the estimated AOI $\varphi = 27^o$. To eliminate false edges, the results were 'fine-tuned' by the alignment procedure described above. The results shown in the top row of Fig. 7 can be compared with the "ground-truth" shown in the bottom row of this figure.

5. Discussion

Real and virtual objects superimposed by a reflecting surface can be well separated and labeled by the proposed method. The method significantly extends the useful range of incidence angles for polarization-based clearing of transparent disturbances. In addition, it automatically provides the inclination of the invisible surface that lies between the camera and the visible objects. It may be a basis for useful and practical techniques in amateur and professional photography, and enable scene understanding in the presence of semi reflections.

We believe that mutual information may be a better measure than decorrelation for correct separation, especially

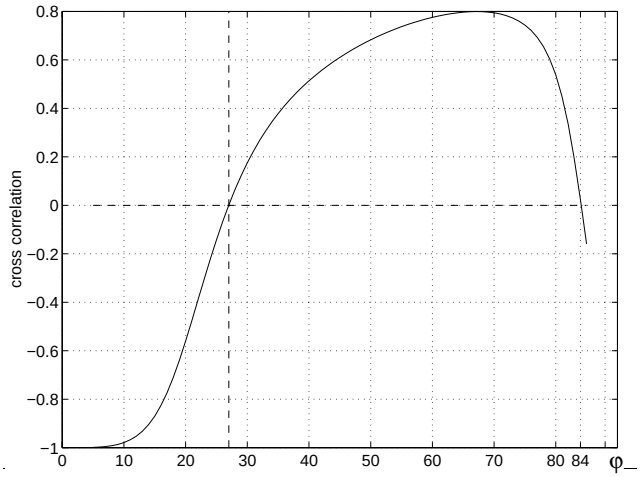

Figure 6. At the estimated angle 27^o the estimated layers are decorrelated.

Figure 7. [Top row]: The reconstructed real (left) and virtual (right) layers, based on the automatic detection of the angle of incidence. [Bottom left]: The real object photographed without the interfering glass window. [Bottom right]: The virtual object photographed by removing the objects behind the glass window.

when there is some correlation between the scenes, or when the scene contains opaque objects beside transparent ones. This measure is being studied. Other issues we consider are the effects of noise and curvature of the reflecting surface across the field of view. The observed objects may partially polarize the light before its incidence on the semi-reflecting medium (e.g., by specular reflections from dielectrics). We expect this to somewhat degrade the performance of the current method, motivating further improvements in the approach.

This research was carried out in the Ollendorff Center of the Department of Electrical Engineering, Technion, and in the Department of Electrical Engineering - Systems, Faculty of Engineering, Tel-Aviv University. It was funded in part by the Israeli Ministry of Science.

References

[1] M. Born and E. Wolf, *Principles of optics*, 5th ed., (Pergamon, Oxford, 1975).

[2] J. R. Bergen, P. J. Burt, R. Hingorani and S. Peleg, "Transparent motion analysis" Proc. ECCV, pp. 566-569, 1990.

[3] H. Farid and E. H. Adelson, "Separating reflections and lighting using independent components analysis," Proc. CVPR, Vol-I, pp. 262-267, 1999.

[4] H. Fujikake, K. Takizawa, T. Aida, H. Kikuchi, T. Fujii and M. Kawakita, "Electrically-controllable liquid crystal polarizing filter for eliminating reflected light," Optical Review **5**, pp. 93-98, 1998.

[5] S. K. Nayar, X. S. Fang and T. Boult, "Separation of reflection components using color and polarization," Int. J. Comp. Vis. **21**, pp. 163-186, 1997.

[6] N. Ohnishi, K. Kumaki, T. Yamamura and T. Tanaka, "Separating real and virtual objects from their overlapping images," Proc. ECCV, Vol-II, pp. 636-646, 1996.

[7] M. Oren and S. K. Nayar, "A theory of specular surface geometry," Proc. ICCV, pp. 740-747, 1995.

[8] Y. Y. Schechner, N. Kiryati and R. Basri, "Separation of transparent layers using focus," Proc. ICCV, pp. 1061-1066, Mumbai, 1998.

[9] M. Shizawa, "On visual ambiguities due to transparency in motion and stereo," Proc. ECCV, pp. 411-419, 1992.

[10] W. A. Shurcliff and S. S. Ballard, *Polarized light* (Van Nostrand, Princeton, 1964).

[11] R. Walraven, "Polarization imagery," Opt. Eng. **20**, pp. 14-18, 1981.

[12] D. Weinshall, "Perception of multiple transparent planes in stereo vision," Nature **341**, pp. 737-739, 1989.

[13] L. B. Wolff, "Using polarization to separate reflection components," Proc. CVPR, pp. 363-369, 1989.

[14] L. B. Wolff, "Polarization vision: a new sensory approach to image understanding," Image and Vision Computing **15**, pp. 81-93, 1997.